

Figure 3. Four geometries.

3. Results and discussion

In this section sample calculations are carried out to demonstrate the effects of specular reflective boundary conditions on Discrete Ordinate Methods solutions. The boundary condition may be used for periodic or symmetry geometries. In the first example, the consistency is demonstrated.

3.1. An axisymmetric and periodic example

An axisymmetric radiation problem is considered here to demonstrate that the proposed boundary condition produces identical results as those from the full geometry. A homogeneous emitting–absorbing medium is confined in an infinitely long cylindrical enclosure bounded by black and cold walls. The problem is one-dimensional in the radial direction, and has two symmetry conditions. One is along the azimuthal direction, the other one is along the axial direction. The problem therefore may be solved with four different geometries as shown in Fig. 3. Geometry A is a sufficiently long cylinder bounded by black and cold walls at both ends. The radial cross section at the center achieves the target solution asymptotically as the length of the cylinder increases. Specularly reflective boundary conditions, therefore, are not needed in this geometry. Geometry B has a wedge shape with one layer of cells along the azimuthal direction, and takes advantage of the axisymmetry of the problem. Both of the additional front and back surfaces require the specular reflective boundary condition. Geometry C has a pie shape with only one layer of cells along the axial direction. It utilizes axial periodicity, such that both up and down surfaces are specularly reflective. Finally, Geometry D utilizes both axial periodicity and axisymmetry, and has cells only along the radial direction. Specularly reflective boundaries are applied to front, back, top and bottom surfaces. Because the solution (e.g., incident radiation or radiative heat source) of this problem has only radial variations, a successful boundary condition for the reduced geometries should produce identical results in all four geometries.

In all four geometries, a cylindrical grid with uniform spacing along axial, radial and azimuthal directions is used to discretize the RTE. The wedge geometries (Geometry B and D) have a 10° angle. Geometry A and C have 36 azimuthal cells with 10° for each wedge. Geometry A and B have 100 uniform axial cells, and Geometry C and D have identical height corresponding to the cell height in Geometry A and B. A total of 72 ordinates (2 polar and 36 azimuthal directions) are employed. The choice of large number of azimuthal direction ensures that the reflected ordinate is within the set of ordinates. The radial direction is uniformly discretized into 1000 cells. The radius of the cylinder is 1 m, and the absorption coefficient is 1 cm^{-1} ; emission is homogeneous.

The solutions for normalized incident radiation ($G/4\pi I_b$) are compared in Fig. 4 with the exact results. Results from all four geometries overlap with each other, demonstrating the effectiveness of the proposed specular reflective boundary condition in dealing with both axisymmetric and periodic symmetries. The computational costs are 16720, 158, 15, and 2 seconds for Geometry A to D, respectively. A significant reduction of computational cost is achieved.

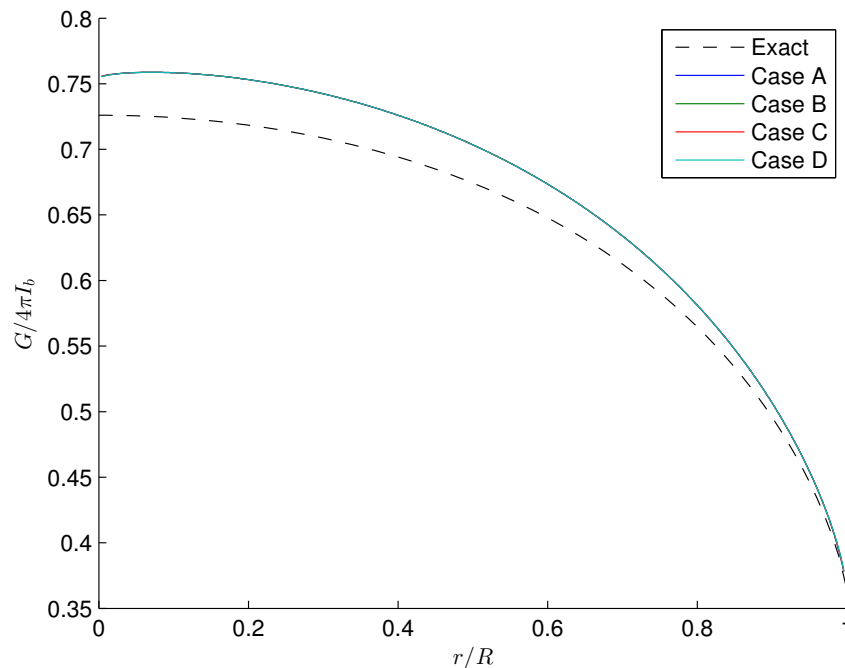


Figure 4. Comparison of the normalized incident radiation predicted from four geometries.

3.2. Axisymmetric jet flame

The specular reflective boundary condition is further applied to an axisymmetric jet diffusion flame solved on a wedge mesh similar to Geometry B in Fig. 3. The flame was derived from the methane–air partially premixed Sandia Flame D [10] by artificially quadrupling the jet diameter [11, 12] to make radiation in this small laboratory-scale flame appreciable. The wedge mesh has a 10° opening angle. Time-averaged profiles are used for the radiation calculations. The same flame was previously employed to investigate the accuracy and efficiency of k -distribution methods and P_N RTE solvers [13]. In this section the results from Discrete Ordinate Methods are reported. The spectral model is the full-spectrum k -distribution method assembled from a narrowband k -distribution database [14]. The polar direction is aligned with the axial direction. 36 azimuthal ordinates are employed so that reflected ordinates are also contained within the set of ordinates; the numbers of polar directions vary from 2 to 32.

The radiative heat flux divergence ($\nabla \cdot \mathbf{q}$), i.e., the negative of the radiative heat source in the energy equations predicted by different DOM implementations are compared with PMC and P_1 at 1 m and 1.43 m above the nozzle in Figs. 5 and 6, respectively. Radiative emission is determined by the Optically Thin approximation (OT). The true radiative heat sources are determined by PMC coupled with a line-by-line spectral model. Identical trends are found at both downstream locations. The P_1 model recovers most of the non-gray self-absorption when coupled with the full-spectrum k -distributions. DOM with 2 polar ordinates overpredicts absorption, increasing the number of polar ordinates improves the accuracy only slightly, and the amount of improvement is small compared to the overall amount of self-absorption. Therefore, DOM results from different ordinate configurations appear very close.

3.3. Conclusions

In this work, a specular reflective boundary condition similar to that employed in Photon Monte Carlo method is proposed to reduce computational geometry by exploring periodicity or symmetry of the problem. The expression of the boundary condition depends on the spatial discretization scheme for the divergence term. For the simplest step scheme, the specular reflective boundary condition for ordinate intensity reduces to zero gradient (or fixed value) for incoming (or outgoing) directions relative to the boundary. Therefore, the intensity of outgoing ordinate at the boundary after reflection depends on the intensity of the incoming ordinate, but not vice versa. However, for higher order schemes the incoming